Physiologically Based Pharmacokinetics of Digoxin in *mdr*1a Knockout Mice

MASAMI KAWAHARA,[†,‡] ATSUSHI SAKATA,[†] TOSHIAKI MIYASHITA,[†] IKUMI TAMAI,[†,§] AND AKIRA TSUJI*[,†,§]

Contribution from *Faculty of Pharmaceutical Sciences, Kanazawa University, 13-1 Takara-machi, Kanazawa 920-0934, Japan, and CREST, Japan Science and Technology Corporation, 4-1-8 Hon-machi, Kawaguchi 332-0012, Japan.*

Received June 4, 1999. Final revised manuscript received September 28, 1999.
Accepted for publication October 5, 1999.

Abstract □ To determine the contribution of the *mdr*1a gene product to digoxin pharmacokinetics, we constructed a physiologically based pharmacokinetic model for digoxin in *mdr*1a (–/–) and *mdr*1a (+/+) mice. After intravenous administration, total body clearance and tissue-to-plasma concentration ratios for muscle and heart were decreased in *mdr*1a (–/–) mice as compared with *mdr*1a (+/+) mice, and in particular, the digoxin concentration in the brain was 68-fold higher than that in *mdr*1a (+/+) mice at 12 h. On the other hand, *mdr*1a gene disruption did not change the contributions of renal and bile clearances to total clearance, the plasma protein binding, or the blood-to-plasma partition coefficient. Brain concentration–time profiles in *mdr*1a (+/+) and *mdr*1a (–/–) mice showed a different pattern from those in plasma and other tissues, indicating digoxin accumulation in the brain tissue. Because there was no difference in the uptake or release of digoxin by brain tissue slices from the two types of mice, we assumed the brain tissue compartment to consist of two parts (a well-stirred part with influx and efflux clearance and an accumulative part). Simulation with this model gave excellent agreement with observation when active efflux clearance across the blood–brain barrier was assumed to be zero in *mdr*1a (–/–) mice. The observations in other tissues in both types of mice were also well simulated.

Introduction

The *MDR*1 gene encodes human P-glycoprotein. In mice, two P-glycoproteins (encoded by the *mdr*1a and *mdr*1b genes) appear to perform the function of the single human protein.[1−5] The tissue distribution of these two isoforms in the mouse is different but partly overlapping. The mouse *mdr*1a gene is predominantly expressed in the intestine, liver, and capillary endothelial cells of brain and testis, whereas the *mdr*1b gene is predominantly expressed in the adrenal, placenta, ovary, and pregnant uterus.[3,6] Similar levels of *mdr*1a and *mdr*1b expression are found in the kidney. Schinkel et al. reported that the absence of the *mdr*1a P-glycoprotein has a pervasive influence on the tissue distribution and pharmacokinetics of drugs such as ivermectin, vinblastine, cyclosporin A, digoxin, etc.[7,8] The most striking effects were observed in the brain, owing to the high level of *mdr*1a P-glycoprotein at the blood−brain barrier. The use of *mdr*1a (−/−) mice allowed us to investigate pharmacokinetically the in vivo function of P-glycoprotein.

Digoxin is widely used in the treatment of congestive heart failure and is a substrate of P-glycoprotein.[9] Schinkel et al. reported a 35-fold higher concentration of digoxin in *mdr*1a (−/−) mouse brain than in *mdr*1a (+/+) mouse brain 4 h after intravenous administration.[8] They also suggested that the pharmacokinetics of digoxin in *mdr*1a (−/−) mice was quite different from that in *mdr*1a (+/+) mice. Mayer et al. also found that the brain level of [^{3}H]digoxin in *mdr*1a (−/−) mice continuously increased over a period of 3 days, resulting in a 200-fold higher concentration than in *mdr*1a (+/+) mice.[10] Clinically, digoxin may be coadministrated with other drugs which potentially inhibit P-glycoprotein in the treatment of cancer in elderly patients, and this may lead to dangerous side effects of digoxin, including nausea, tremor, or heart failure.

In this study, we investigated the pharmacokinetics of digoxin in *mdr*1a (−/−) mice by modifying the physiologically based pharmacokinetic model in rats reported by Harrison and Gibaldi,[11] in order to reveal the role of the *mdr*1a gene product in relation to tissue distribution and renal or biliary clearance. In particular, we tried to simulate the change of brain digoxin concentration due to loss of active efflux across the blood−brain barrier in *mdr*1a (−/−) mice.

Materials and Methods

Chemicals—[^{3}H]Digoxin (555 GBq/mmol) and SOLVABLE were obtained from New England Nuclear (Boston, MA), digoxin from Sigma Chemical Co. Ltd. (St. Louis, MO), and Clear-sol I, a liquid scintillation fluid, from Nacarai-Tesque Inc. (Kyoto, Japan). Other drugs and chemicals were commercial products.

Animals—Male *mdr*1a (−/−) mice (body weight 25−30 g) were obtained from Taconic Farms Inc. (Germantown, NY). Male C57BL/6 mice (body weight 25−30 g) obtained from Sankyo Laboratory Co. Ltd. (Hamamatsu, Shizuoka, Japan) were used as the control mice because genetically compatible wild-type *mdr*1a (+/+) mice, F2 and F3 generations of 129/Ola and FVB mice, were not available in Japan at the time when we started this study. We confirmed in a preliminary study that male C57BL/6 mice showed similar disposition kinetics of several drugs, P-glycoprotein substrates including tacrolimus, digoxin, and cyclosporin A, to the wild-type (+/+) mice (data not shown). Animals were maintained with free access to water and food in an air-conditioned room in the Institute for Experimental Animals, Faculty of Medicine, Kanazawa University.

Digoxin Pharmacokinetic Study—[^{3}H]Digoxin at 1 mg/kg (2.96 MBq/kg, 0.5 mg/mL in 40% ethanol solution) was administered to each mouse via a 29 G syringe into a jugular vein. At each sampling time, a midline incision was made under ether anesthesia, and whole blood was taken into a heparin-coated syringe from the inferior vena cava. Blood samples were centrifuged at 12 000 rpm for 3 min to obtain plasma. Brain, heart, liver, kidney, and muscle were isolated, washed in ice-cold saline, and then weighed. The contents of the intestine were removed and washed in ice-cold saline. About 0.1 g of each tissue was weighed and then dissolved by vibration (100 strokes/min) in SOLVABLE

* Author to whom correspondence should be addressed. Tel: +81-76-234-4479. Fax: +81-76-234-4477. E-mail: tsuji@kenroku.kanazawa-u.ac.jp.
† Faculty of Pharmaceutical Sciences, Kanazawa University.
‡ Present address: Hospital Pharmacy, School of Medicine, Kanazawa University, 13-1 Takara-machi, Kanazawa 920-8641.
§ CREST, Japan Science and Technology Corporation.

10.1021/js9901763 CCC: $18.00
Published on Web 11/06/1999

at below 60 °C for 2 h. After decolorization with H_2O_2, Clear-sol I and 5 N HCl were added, and the radioactivity was measured with a liquid scintillation counter (LSC-3500, ALOKA, Tokyo, Japan).

Tissue Slice Uptake Study—Preparation of tissue slices for uptake or release experiments was performed according to Gutierrez and Delgadoo-Coello.[12] Brain or skeletal muscle was collected from the completely bled mouse and was sliced with a razor blade 5−8 mm in diameter and 0.2−0.5 mm in thickness, in ice-cold Krebs-Ringer's Tris buffer (pH 7.4). Tissue slices weighing 5−20 mg were preincubated at 37 °C for 10 min in the presence or absence of 500 μM ouabain with continuous bubbling with 95% O_2/5% CO_2. Uptake experiments were started by replacing the buffer with [^{3}H]digoxin (7 nM)-containing buffer in the presence or absence of ouabain (500 μM). To terminate the uptake, tissue slices were washed three times with ice-cold buffer and solubilized with 5% sodium dodecyl sulfate in the counting vial, then Clear-sol I was added, and the radioactivity was measured with a liquid scintillation counter. Release experiments were carried out in a similar way, preincubation was done at 37 °C for 90 min in the buffer solution containing [^{3}H]digoxin, and then the buffer solution was exchanged for digoxin-free buffer at the starting time for the release study.

Plasma Protein Binding and Blood-to-Plasma Partition Coefficient—Plasma-free fraction of digoxin was measured by ultrafiltration. Two and one-half microliters of 40% ethanol solution containing [^{3}H]digoxin was added to 100 μL of plasma obtained from mice to produce a final concentration of 0.1−1000 ng/mL. After incubation at 37 °C for 30 min, samples were filtered with a Centrifree (Amicon Inc., Beverly, MA) at 1000 g, 37 °C for 10 min. Digoxin-free fraction was calculated according to the equation

$$f_p = C_f/C_p$$

where f_p, C_f, and C_p are digoxin-free fraction in the plasma, concentration of free digoxin in plasma calculated from the radioactivity in the filtrate, and total digoxin concentration in plasma, respectively.

Blood-to-plasma partition coefficient (R_B) was measured in vivo. One milliliter of blood samples was collected at 4 and 12 h after administration of [^{3}H]digoxin at 1 mg/kg (2.96 MBq/kg, 0.5 mg/mL in 40% ethanol solution). The blood sample was divided into two parts. One part was solubilized with SOLVABLE. The other part was centrifuged at 12 000 rpm for 3 min, and the radioactivity in solubilized whole blood and plasma was measured. The value of R_B was calculated as follows:

$$R_B = C_{blood}/C_p$$

where C_{blood} and C_p are digoxin concentrations in whole blood and in plasma, respectively.

Measurement of Renal and Bile Clearances—To determine the renal and bile clearances, mice were midline-incised and the renal artery or bile duct was ligated under ether anesthesia according to Harrison and Gibaldi.[11] [^{3}H]Digoxin was injected at a dose of 1 mg/kg (2.96 MBq/kg, 0.5 mg/mL in 40% ethanol solution), and the blood was sampled at 0.25, 0.5, 1, 2, and 4 h after the administration. Plasma samples were obtained by centrifugation at 12 000 rpm for 3 min, and then the radioactivity was measured with a liquid scintillation counter. Bile clearance was calculated from the difference between total clearance and the clearance obtained in bile-duct-ligated mice. Renal clearance was calculated from the difference between total clearance and the clearance obtained in renal-artery-ligated mice.

Physiologically Based Pharmacokinetic Model—A physiologically based pharmacokinetic model was constructed according to Harrison and Gibaldi,[11] including enterohepatic recirculation. As shown in Figure 1, the brain compartment was additionally modified in this study for investigation of the influence of *mdr*1a gene disruption. Since the digoxin plasma concentration−time profile was assumed to be biexponential up to 4 h (see Figure 2), we predetermined the pharmacokinetic parameters between plasma and brain with a hybrid model shown in Figure 3. In this hybrid model analysis, it was assumed that the drug penetrates by passive diffusion bidirectionally in both types of mice and is actively excluded by P-glycoprotein from the brain only in *mdr*1a (+/+) mice. The passive diffusion was defined as uptake clearance, and the efflux by P-glycoprotein was defined as efflux clearance

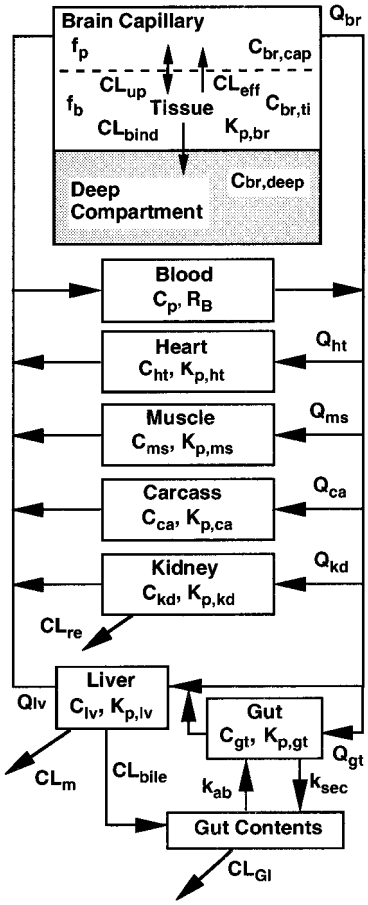

Figure 1—Physiologically based pharmacokinetic model for digoxin in mice: Q_i, CL_i, C_i and $K_{p,i}$ represent plasma flow rate, clearance, tissue drug concentration, and tissue-to-plasma concentration ratio for tissue i, respectively. The brain compartment was divided into three parts; CL_{up}, CL_{eff}, and CL_{bind} are the uptake clearance by passive diffusion, the efflux clearance by P-glycoprotein, and the binding clearance by accumulation, respectively.

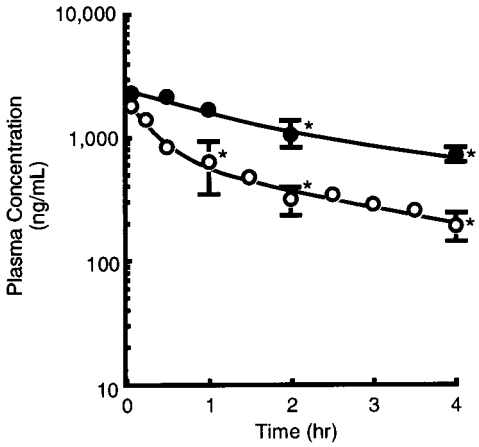

Figure 2—Plasma concentration–time profiles of [^{3}H]digoxin after 1 mg/kg intravenous administration in *mdr*1a (+/+) and *mdr*1a (–/–) mice. Drug solutions were administered to the lightly anesthetized *mdr*1a (+/+) and *mdr*1a (–/–) male mice via a jugular vein. Plasma concentrations were determined from the radioactivity. Open (○) and closed (●) symbols represent the results obtained in *mdr*1a (+/+) mice and *mdr*1a (–/–) mice, respectively (n = 3–5 for points marked with an asterisk (*); n = 1 for other points).

in this study. Two steps were taken in this determination. (1) The brain concentration−time profile in *mdr*1a (−/−) mice was simulated by means of the Runge−Kutta−Gill integration method using the hybrid model which employed a least-squares biexponential fitting to the plasma concentration−time profile. (2) The efflux clearance was estimated from the brain concentration−time

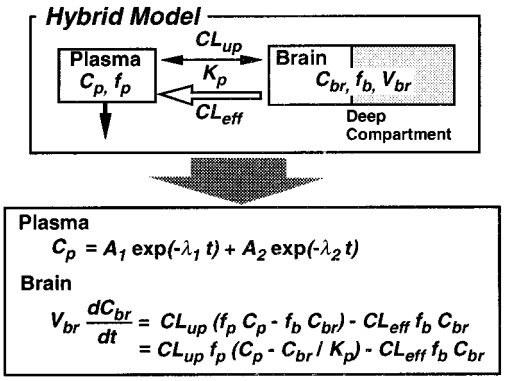

Figure 3—Hybrid pharmacokinetic model for brain distribution of drugs excluded by an active efflux system in mice. This model was employed for estimation of the values of CL_{up} and CL_{eff} in the brain under the condition that the distribution volume of brain was too small to affect significantly the systemic disposition of a test drug. In this model, it was assumed that the drug penetrates by passive diffusion with an uptake clearance (CL_{up}) bidirectionally in both types of mice and is actively excluded with an efflux clearance (CL_{eff}) by P-glycoprotein from the brain tissue only in *mdr*1a (+/+).

Table 1—Pharmacokinetic Parameters for Digoxin after 1 mg/kg Intravenous Administration in *mdr*1a (+/+) and *mdr*1a (–/–) Mice

	*mdr*1a (+/+)	*mdr*1a (–/–)
AUC (μg·min/mL)	155.4	439.8
MRT (min)	169.2	214.8
CL_{tot} (mL/min/kg)	6.44	2.27
V_d (L/kg)	1.09	0.488

profile in *mdr*1a (+/+) mice. Recently, Chen and Pollack have reported the simulation study of pharmacokinetics–pharmacodynamics of [D-penicillamine[2,5]]enkephalin[13] by a similar manner in *mdr*1a (–/–) mice.

As reported by Schinkel et al. the brain digoxin concentration in *mdr*1a (–/–) mice was very much higher than those in other tissues at 4 h after the administration.[8] Digoxin seems to be accumulated in brain tissue in *mdr*1a (–/–) mice. Then, the brain compartment was divided into three parts. The first compartment is brain capillary, the second is well-stirred brain tissue (interstitial fluid and intracellular space), and the third is a digoxin strongly binding deep compartment. The accumulation clearance to the deep compartment was determined by trial-and-error simulation.

Differential equations (see Appendix) were solved simultaneously by a FACOM-M776/20 in Kanazawa University Information Processing Center.

Results

Plasma Concentration–Time Profiles of Digoxin in *mdr*1a (+/+) and *mdr*1a (–/–) Mice—Figure 2 shows the plasma concentration–time profiles of digoxin after 1 mg/kg intravenous administration in *mdr*1a (+/+) and *mdr*1a (–/–) mice. Pharmacokinetic parameters were determined by moment analysis and are listed in Table 1. In *mdr*1a (–/–) mice, total clearance of digoxin was decreased to 30% of that in *mdr*1a (+/+) mice, and the distribution volume was also decreased to 50%. We also studied antipyrine plasma concentration–time profiles, which is considered as a marker of passive diffusion; there was no difference in these parameters between *mdr*1a (+/+) and *mdr*1a (–/–) mice (data not shown).

Tissue Distribution Study—Plasma and tissue digoxin concentration–time profiles were measured after 1 mg/kg administration in *mdr*1a (+/+) and *mdr*1a (–/–) mice. Tissue-to-plasma concentration ratios (K_p) were determined from the elimination phase according to Chen and Gross.[14] As shown in Table 2, K_p values of heart, muscle, intestine, and carcass were decreased largely in *mdr*1a (–/–) mice, being about half of those in *mdr*1a (+/+) mice. On the other hand, the K_p values of kidney and liver were slightly changed.

Table 2—Tissue-to-Plasma Concentration Ratios of Digoxin in *mdr*1a (+/+) and *mdr*1a (–/–) Mice

	*mdr*1a (+/+)	*mdr*1a (–/–)
brain	9.4	*a*
heart	1.13	0.626
muscle	0.804	0.424
kidney	1.07	0.797
liver	1.87	2.09
intestine	2.59	0.535
carcass	1.12	0.309

[a] K_p value of *mdr*1a (–/–) mice could not be determined by the method of Chen and Gross,[14] because it failed to reach the terminal phase.

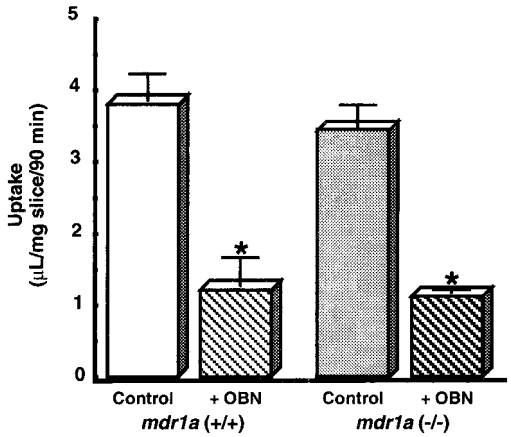

Figure 4—Effect of ouabain on the uptake of digoxin by brain slices from *mdr*1a (+/+) and (–/–) mice. Both types of mice were decapitated, and the brains were isolated and sliced with a razor blade in ice-cold buffer. The slices were preincubated at 37 °C for 10 min in the absence or presence of ouabain (500 μM), and then the uptake of [^{3}H]digoxin (7 nM) was measured for 90 min. Each column represents the mean ± SEM ($n = 4$). (*) Significantly different from control *mdr*1a (+/+) mice by Student's *t*-test ($p < 0.05$).

Brain and Muscle Slice Uptake Study—To clarify whether the changes in K_p values are related to the participation of P-glycoprotein, tissue binding, or other factors, an uptake study with brain and muscle slices was carried out.

As shown in Figure 4, there was no significant difference between digoxin uptake by brain slices of the two types of mice. In the presence of 500 μM ouabain, which completely inhibits digoxin binding to Na^+/K^+-ATPase, digoxin uptake was decreased to 30% of the control. It is likely that uptake clearance and binding of digoxin in the brain are not affected by the *mdr*1a gene product. The release of digoxin from brain slices was also at the same level in both types of mice. Although approximately 90% of digoxin still remained after 60 min, the amounts were decreased to 50% in the presence of 500 μM ouabain (data not shown). The brain digoxin concentration in *mdr*1a (+/+) mice was little changed at 12 h after administration in vivo, while the plasma digoxin concentration was decreased. These results strongly suggest that digoxin accumulation in the brain tissue results from binding of the drug with Na^+/K^+-ATPase, the contribution of which was estimated from the in vitro uptake study to account for approximately 70% of total brain digoxin concentration.

As shown in Figure 5, digoxin uptake by muscle slices was significantly decreased in *mdr*1a (–/–) mice, being about half of that in *mdr*1a (+/+) mice. This is the same as the in vivo distribution, indicating that the distribution

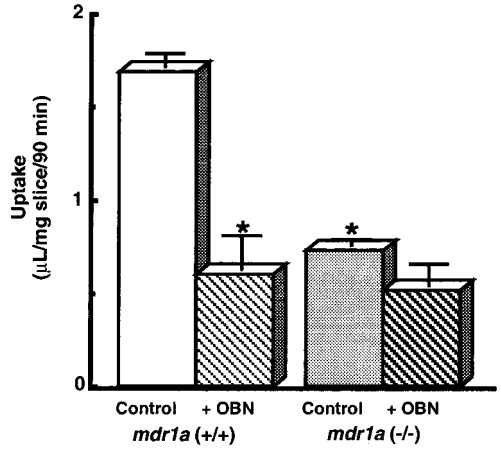

Figure 5—Effect of ouabain on the uptake of digoxin by muscle slices from *mdr*1a (+/+) and (–/–) mice. Muscle slices from both types of mice were preincubated at 37 °C for 10 min in the absence or presence of ouabain (500 μM), and then the uptake of [^{3}H]digoxin (7 nM) was measured for 90 min. Each column represents the mean ± SEM ($n = 4$). (*) Significantly different from control *mdr*1a (+/+) mice by Student's *t*-test ($p < 0.05$).

Table 3—Renal and Bile Clearances in *mdr*1a (+/+) and *mdr*1a (–/–) Mice[a]

clearance	*mdr*1a (+/+) (mL/min/kg)	*mdr*1a (–/–) (mL/min/kg)
CL_{tot}	5.64 (100)	1.91 (100)
CL_{re}	3.15 (55.9)	0.99 (51.8)
CL_{bile}	2.30 (40.8)	0.84 (44.0)
CL_m	0.19 (3.4)	0.08 (4.2)

[a] Renal and bile clearances of both types of mice were determined from the decrease in apparent total clearance in renal-artery-ligated and bile-duct-ligated mice, respectively. Percentage contributions to total clearance are shown in parentheses. Metabolic clearance was assumed to be residual clearance.

volume has decreased in *mdr*1a (−/−) mice. Digoxin uptake by muscle slices of both types of mice was decreased to the same level in the presence of 500 μM ouabain. Approximately 80% of digoxin was released after 60 min (data not shown).

Plasma-Free Fraction and Blood-to-Plasma Partition Coefficient of Digoxin—Plasma-free fraction (f_p) of digoxin was estimated to be about 0.78 in both types of mice, and there was no significant change with digoxin concentration from 0.1 to 1000 ng/mL. The R_B values of *mdr*1a (+/+) and *mdr*1a (−/−) mice were 0.898 ± 0.040 and 0.883 ± 0.033 ($n = 5-6$, mean ± SEM), respectively. These results suggest that plasma protein binding and binding to blood cells were not affected by the *mdr*1a gene product.

Estimation of Renal and Bile Clearances—To determine the contributions of renal and bile clearances, 1 mg/kg digoxin was administered intravenously to renal artery- or bile-duct-ligated mice. Renal or bile clearance was estimated from the difference from total clearance, and the results are listed in Table 3. Renal and bile clearances were 55.9% and 40.8% of total clearance in *mdr*1a (+/+) mice, and 51.8% and 44.0% in *mdr*1a (−/−) mice, respectively. In *mdr*1a (−/−) mice, total clearance was decreased to 30% of the control, while there was little change in the contribution of renal and bile clearances to total clearance.

Plasma, urine, and bile samples were analyzed by high-performance liquid chromatography. No metabolite was detected by HPLC in urine, bile, or plasma. Metabolic clearance in both types of mice seems to be very small. Furthermore, as shown in Table 3, the sum of renal and biliary clearances was nearly equal to the total clearance in both types of mice, supporting the above findings.

Physiologically Based Pharmacokinetic Model for Digoxin in Mice—After the determination of renal and bile clearances, enterohepatic clearances were estimated. GI tract clearance was estimated by scaling down from the data reported by Harrison and Gibaldi for rats.[11] The absorption and secretion rate constants were assumed to be the same as those in rats. In *mdr*1a (−/−) mice, the secretion clearance was assumed to be zero, because there was no P-glycoprotein expression in the small intestine of *mdr*1a (−/−) mice.

The brain digoxin concentration−time profile showed a quite different pattern from that of plasma. In *mdr*1a (+/+) mice, the brain digoxin concentration increased rapidly after administration and then decreased slowly after 4 h. In *mdr*1a (−/−) mice, the brain digoxin concentration increased slowly to a plateau. Therefore, the brain digoxin pharmacokinetics was considered to be complex. Because this phenomenon could not be described by a uniform compartment, the brain compartment was divided into three parts. The first is the capillary blood space compartment, the second is the well-stirred interstitial and intracellular compartment, and the third is the digoxin strongly binding compartment (deep compartment). The volumes of the capillary blood space and interstitial fluid or brain tissue were taken from the literature. Since the amount of digoxin uptake by brain slices decreased to 30% of the control in the presence of ouabain, the Na^+/K^+-ATPase-related binding space was estimated to be about 70% of brain tissue volume. Estimated uptake and efflux clearances (see Figure 3) were 2.5 μL/min and 0.4 mL/min, the accumulation clearance to the deep compartment was 0.1 μL/min determined by trial-and-error simulation. All parameters used in this pharmacokinetic model are listed in Table 4.

Finally, plasma and tissue digoxin concentration−time profiles in both types of mice were simulated according to the physiologically based model illustrated in Figure 1 and in the Appendix, and the results are shown in Figure 6a,b. All tissues and plasma concentration−time profiles up to 12 h after administration were well predicted.

Discussion

We have shown here that the conspicuous difference of brain digoxin concentration between *mdr*1a (−/−) and (+/+) mice can be simulated with this physiologically based model. It is noteworthy that the efflux clearance determines the distinctive pharmacokinetics of digoxin in *mdr*1a (−/−) mice. P-Glycoprotein in the kidney and liver acts as a secretion pump, while it acts as an absorption barrier or efflux pump in the small intestine for a variety of structurally unrelated hydrophobic and neutral or cationic compounds, including many cytotoxic drugs, and also as a transporter of steroid hormones in the adrenals and placenta.[9,15−23] Furthermore, P-glycoprotein in brain capillary endothelial cells acts as a blood−brain barrier to lipophilic drugs.[1,24−30] As P-glycoprotein is expressed in almost all tissues of the body, the absence of P-glycoprotein may cause remarkable changes in drug pharmacokinetics. In fact, Schinkel et al. reported that the pharmacokinetics of substrates of P-glycoprotein was changed in several tissues and dramatically in the brain of *mdr*1a (−/−) mice.[7,8]

Schinkel et al. reported that there are no physiological abnormalities in *mdr*1a (−/−) mice.[7] We also confirmed that the plasma protein binding, blood-to-plasma partition ratio, and metabolic feature of digoxin were the same in both types of mice. However, the digoxin concentration in the brain of *mdr*1a (−/−) mice was markedly increased, owing to the absence of efflux clearance via P-glycoprotein at the blood−brain barrier. Moreover, the digoxin concen-

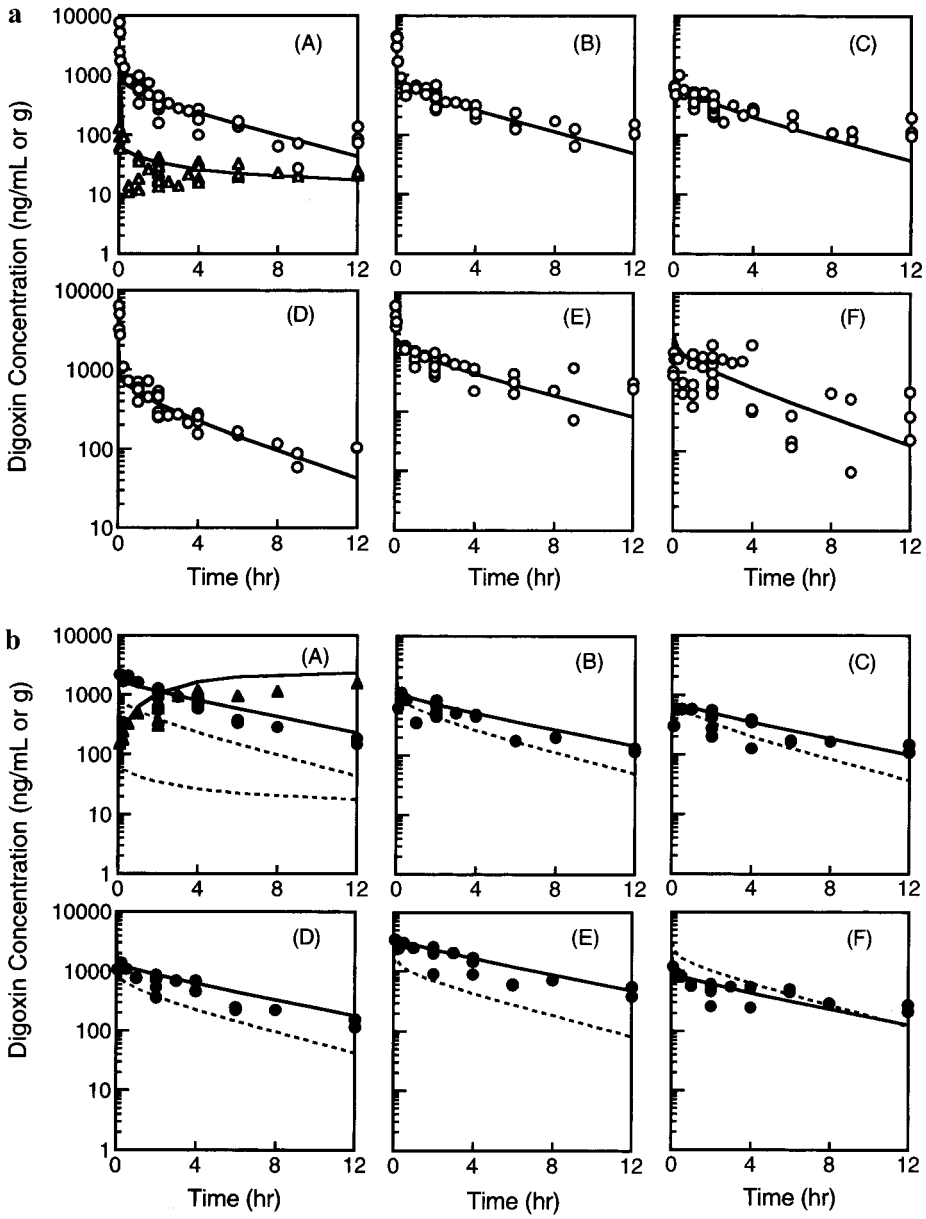

Figure 6—(a) Predicted and observed plasma and tissue concentrations of digoxin in *mdr*1a (+/+) mice after 1 mg/kg intravenous administration: (A) plasma (○), brain (△), (B) heart, (C) muscle, (D) kidney, (E) liver, and (F) gut. Solid lines represent the simulation curves from the physiologically based pharmacokinetic model. (b) Predicted and observed plasma and tissue concentrations of digoxin in *mdr*1a (–/–) mice after 1 mg/kg intravenous administration. (A) plasma (●), brain (▲), (B) heart, (C) muscle, (D) kidney, (E) liver, and (F) gut. Solid and dashed lines represent the simulation curves for *mdr*1a (–/–) mice and for *mdr*1a (+/+) mice, respectively.

tration in the brain of both types of mice remained high after 4 h. This phenomenon suggests that there is a deep compartment concerned with digoxin accumulation, and this is consistent with the conclusion from the brain slice study that digoxin binds to Na^+/K^+-ATPase.

Mayer et al. reported that urinary excretion of digoxin in *mdr*1a (−/−) mice was increased twice that of *mdr*1a (+/+) mice, and fecal excretion was decreased.[10] More than 16% of the administered digoxin was directly excreted in the intestinal lumen of *mdr*1a (+/+) mice within 90 min and at least 20% of metabolite was excreted in urine in their study. We also reported active secretion from the small intestine in rats.[22] However the contribution of renal clearance to total clearance was little changed in this study. Furthermore, we could not detect any metabolite in urine, bile, or plasma in either type of mouse. The reasons for these differences are unclear, but total radioactivity recovered was almost 100% of initial radioactivity. Although we used literature values for the active secretion and absorption rate constant of the intestine,[11] we could successfully simulate the digoxin pharmacokinetics in *mdr*1a (−/−) mice by neglecting the efflux clearance in the brain and intestine.

Plasma and tissue digoxin concentrations were increased and total body clearance was decreased in *mdr*1a (−/−) mice. However, the K_p values of kidney and liver were little changed. As Schinkel et al. reported that the *mdr*1b gene is up-regulated in liver and kidney of *mdr*1a (−/−) mice,[7] we also observed an increase of *mdr*1b gene expression in those organs (data not shown). This result suggests that digoxin clearance in *mdr*1a (−/−) mice may be supported by the up-regulated *mdr*1b gene in these organs.

In conclusion, we constructed a physiologically based pharmacokinetic model of digoxin in mice by adding a subdivided brain compartment based on the model of Harrison and Gibaldi in rats.[11] Our model could simulate the pharmacokinetics of digoxin in all tissues of *mdr*1a (+/+) and *mdr*1a (−/−) mice. The difference of the brain

Table 4—Pharmacokinetic Parameters for Digoxin in *mdr*1a (+/+) and *mdr*1a (–/–) mice[a]

clearance (mL/hr)	*mdr*1a (+/+)	*mdr*1a (–/–)
CL_{tot}[b]	7.44	2.52
CL_{re}[b]	4.16	1.31
CL_{bile}[b]	3.04	1.11
CL_m[b]	0.25	0.11
CL_{GI}[c]	0.019	0.019
k_{ab}[c,d]	0.036	0.036
k_{sec}[c,d]	0.72	

	Volume[e] (mL)	Blood Flow[e] (mL/min)
blood	1.0	4.38
heart	0.10	0.28
liver	1.30	1.10
kidney	0.34	0.80
intestine	1.50	0.90
muscle	10.0	0.50
gut contents	0.8	
carcass	6.9	1.61
brain capillary	0.025	0.089
brain tissue	0.068	
deep compartment	0.158	

[a] All parameters were estimated for mice with 22.0 g body weight. [b] Measured. [c] Estimated from ref 11. [d] Rate (h^{-1}). [e] Cited from Mordenti, J., et al. *J. Pharm. Sci.* **1986**, *75*, 1028–1040.

digoxin concentration between *mdr*1a (+/+) and *mdr*1a (−/−) mice could be explained completely in terms of the existence or absence of efflux clearance at the brain capillaries. Since P-glycoprotein regulates the distribution of digoxin into the brain by active efflux transport, co-administration with P-glycoprotein reversal drugs may cause serious side effects of digoxin.

Appendix

Mass balance equations are listed below.

blood pool:

$$V_p R_B(dC_p/dt) = R_B[(Q_{ht}C_{ht}/K_{p,ht}) + (Q_{ms}C_{ms}/K_{p,ms}) + (Q_{kd}C_{kd}/K_{p,kd}) + (Q_{li}C_{li}/K_{p,li}) + (Q_{ca}C_{ca}/K_{p,ca}) + Q_{br}C_{br,cap}] - R_B Q_{blood} C_p$$

brain capillaries:

$$V_{br,cap}R_B(dC_{br,cap}/dt) = R_B[Q_{br}(C_p - C_{br,cap}) - CL_{up}f_p(C_{br,cap} - C_{br,ti}/K_{p,br}) + CL_{eff}f_b C_{br,ti}]$$

brain tissue:

$$V_{br,ti}(dC_{br,ti}/dt) = CL_{up}f_p(C_{br,cap} - C_{br,ti}/K_{p,br}) - CL_{eff}f_b C_{br,ti} - CL_{bind}C_{br,ti}$$

brain deep compartment:

$$V_{br,deep}(dC_{br,deep}/dt) = CL_{bind}C_{br,ti}$$

heart, muscle, carcass:

$$V_i(dC_i/dt) = R_B Q_i(C_p - C_i/K_{p,i})$$

kidney:

$$V_{kd}(dC_{kd}/dt) = R_B Q_{kd}(C_p - C_{kd}/K_{p,kd}) - CL_{re,int}f_p C_{kd}/K_{p,kd}$$

liver:

$$V_{li}(dC_{li}/dt) = R_B(Q_{li} - Q_{gt})C_p + R_B Q_{gt}C_{gt}/K_{p,gt} - R_B Q_{li}C_{li}/K_{p,li} - (CL_m + CL_{bile,int})f_p C_{li}/K_{p,li}$$

gut wall:

$$V_{gt}(dC_{gt}/dt) = R_B Q_{gt}(C_p - C_{gt}/K_{p,gt}) + k_{ab}C_{gc}V_{gc} - k_{sec}C_{gt}V_{gt}$$

gut contents:

$$V_{gc}(dC_{gc}/dt) = k_{sec}C_{gt}V_{gt} + CL_{bile,int}f_p C_{li}/K_{p,li} - k_{ab}C_{gc}V_{gc} - CL_{GI}C_{gc}$$

where R_B = blood to plasma partition coefficient for digoxin, V_i = volume for tissue i, C_i = concentration for tissue i, Q_i = blood flow rate for tissue i, $K_{p,i}$ = tissue to plasma concentration ratio for tissue i, f_p (f_b) = plasma (tissue) free fraction, k_{ab} (k_{sec}) = absorption (secretion) rate constant, CL_{re} = renal clearance, CL_m = metabolic clearance, CL_{bile} = biliary clearance, CL_{up} = brain tissue uptake clearance, CL_{eff} = brain tissue efflux clearance, CL_{bind} = brain deep compartment binding clearance, and CL_{GI} = GI clearance (fecal clearance).

References and Notes

1. Tsuji, A.; Terasaki, T.; Takabatake, Y.; Tenda, Y.; Tamai, I.; Yamashima, T.; Moritani, S.; Tsuruo, T.; Yamashita, J. P-glycoprotein as the drug efflux pump in primary cultured bovine brain capillary endothelial cells. *Life Sci.* **1992**, *51*, 1427−1437.
2. Thiebaut, F.; Tsuruo, T.; Hamada, H.; Gottesman, M. M.; Pastan, I.; Wilingham, M. C. Cellular localization of the multidrug resistance gene product in normal human tissues. *Proc. Natl. Acad. Sci. U.S.A.* **1987**, *84*, 7735−7738.
3. Croop, J. M.; Raymond, M.; Haver, D.; Devault, A.; Arceci, R. J.; Gros, P.; Housman, D. E. The three mouse multidrug resistance (*mdr*) genes are expressed in a tissue-specific manner in normal mouse tissues. *Mol. Cell. Biol.* **1989**, *9*, 1346−1350.
4. Sugawara, I.; Kataoka, I.; Morishita, Y.; Hamada, H.; Tsuruo, T.; Itoyama, S.; Mori, S. Tissue distribution of P-glycoprotein encoded by a multidrug-resistant gene as revealed by a monoclonal antibody, MRK16. *Cancer Res.* **1988**, *48*, 1926−1929.
5. Cordon-Cardo, C.; O'Brien, J. P.; Casals, D.; Rittman-Grauer, L.; Biedler, J. L.; Melamed, M. R.; Bertino, J. R. Multidrug-resistance gene (P-glycoprotein) is expressed by endothelial cells at blood-brain barrier sites. *Proc. Natl. Acad. Sci. U.S.A.* **1989**, *86*, 695−698.
6. Schinkel, A. H.; Mol, C. A. A. M.; Wagenaar, E.; van Deemter, L.; Smit, J. J. M.; Borst, P. Multidrug resistance and the role of P-glycoprotein knockout mice. *Eur. J. Cancer* **1995**, *31*, 1295−1298.
7. Schinkel, A. H.; Smit, J. J. M.; van Tellingen, O.; Beijnen, J. H.; Wagenaar, E.; van Deemter, L.; Mol, C. A. A. M.; van der Valk, M. A.; Robanus-Maandag, E. C.; te Riele, H. P. J.; Berns, A. J. M.; Borst, P. Disruption of the mouse *mdr*1a P-glycoprotein gene leads to a deficiency in the blood-brain barrier and to increased sensitivity to drugs. *Cell* **1994**, *77*, 491−502.
8. Schinkel, A. H.; Wagenaar, E.; van Deemter, L.; Mol, C. A. A. M.; Borst, P. Absence of the mdr1a P-glycoprotein in mice affects tissue distribution and pharmacokinetics of dexa-

methasone, digoxin, and cyclosporin A. *J. Clin. Invest*. **1995**, *96*, 1698−1705.
9. Tanigawara, Y.; Okumura, N.; Hirai, M.; Yasuhara, M.; Ueda, K.; Kioka, N.; Komano, T.; Hori, R. Transport of digoxin by human P-glycoprotein expressed in a porcine kidney epithelial cell line (LLC-PK1). *J. Pharmacol. Exp. Ther*. **1992**, *263*, 840−845.
10. Mayer, U.; Wagenaar, E.; Beijnen, J.; Smit, J. W.; Mijer, D. K. F.; Asperen, J.; Bornst, P.; Schinkel, A. H.; Substantial excretion of digoxin via the intestinal mucosa and prevention of long-term digoxin accumulation in the brain by the mdr1a P-glycoprotein. *Br. J. Pharmacol*. **1996**, *119*, 1038−1044.
11. Harrison, L. I.; Gibaldi, M.; Physiologically based pharmacokinetic model for digoxin distribution and elimination in the rat. *J. Pharm. Sci*. **1977**, *66*, 1138−1142.
12. Gutierrez, M. C.; Delgado-Coello, B. A.; Influence of pipecolic acid on the release and uptake of [^{3}H]GABA from brain slices of mouse cerebral cortex. *Neurochem. Res*. **1989**, *14*, 405−408.
13. Chen, C.; Pollack, G. M.; Altered disposition and antinociception of [D-Penicillamine^{2,5}]Enkephalin in *mdr*1a-gene-deficient mice. *J. Pharmacol. Exp. Ther*. **1998**, *287*, 545−552.
14. Chen, H.-S. G.; Gross, J. F. Estimation of tissue-to-plasma partition coefficients used in physiological pharmacokinetic models. *J. Pharmacokinet. Biopharm*. **1979**, *7*, 117−125.
15. Borst, P.; Schinkel, A. H.; Smit, J. J. M.; Wagenaar, E.; van Deemter, L.; Smith, A. J.; Eijdems, E. W. H. M.; Bass, F.; Zaman, G. J. R. Classical and novel forms of multidrug resistance and the physiological functions of P-glycoproteins in mammals. *Pharmacol. Ther*. **1993**, *60*, 289−299.
16. Kamimoto, Y.; Gatmaitan, Z.; Hsu, J.; Arias, I. M. The function of Gp170, the multidrug resistant gene product, in rat liver canalicular membrane vesicle. *J. Biol. Chem*. **1989**, *264*, 11693−11698.
17. Speeg, K. V.; Maldonado, A. L.; Liaci, J.; Muirhead, D. Effect of cyclosporine secretion by the kidney multidrug transporter studied in vivo. *J. Pharmacol. Exp. Ther*. **1992**, *261*, 50−55.
18. Hori, R.; Okumura, N.; Aiba, T.; Tanigawara, Y. Role of P-glycoprotein in renal tubular secretion of digoxin in the isolated perfused rat kidney. *J. Pharmacol. Exp. Ther*. **1993**, *266*, 1620−1625.
19. Hsing, S.; Gatmaitan, Z. C.; Arias, I. M. The function of Gp170, the multidrug resistance gene product, in the brush border of rat intestinal mucosa. *Gastroenterology* **1992**, *102*, 879−885.
20. Leu, B. L.; Huang, J. D. Inhibition of intestinal P-glycoprotein and effect on etoposide absorption. *Cancer Chemother. Pharmacol*. **1995**, *35*, 432−436.
21. Hunter, J.; Hirst, B. H.; Simmons, N. L. Drug absorption limited by P-glycoprotein-mediated secretory drug transport in human intestinal epithelial Caco-2 cell layers. *Pharm. Res*. **1993**, *10*, 743−749.
22. Terao, T.; Hisanaga, E.; Sai, Y.; Tamai, I.; Tsuji, A. Active secretion of drugs from the small intestinal epithelium in rats by P-glycoprotein functioning as an absorption barrier. *J. Pharm. Pharmacol*. **1996**, *48*, 1083−1089.
23. Ueda, K.; Okamura, N.; Hirai, M.; Tanigawara, Y.; Saeki, T.; Kioka, N.; Komano, T.; Hori, R. Human P-glycoprotein transports cortisol, aldosterone, and dexamethasone, but not progesterone. *J. Biol. Chem*. **1992**, *267*, 24248−24252.
24. Tsuji, A.; Tamai, I.; Sakata, A.; Tenda, Y.; Terasaki, T. Restricted transport of cyclosporin A across the blood-brain barrier by a multidrug transporter, P-glycoprotein. *Biochem. Pharmacol*. **1993**, *46*, 1096−1099.
25. Tatsuta, T.; Naito, M.; Oh-hara, T.; Sugawara, I.; Tsuruo, T. Functional involvement of P-glycoprotein in blood-brain barrier. *J. Biol. Chem*. **1992**, *267*, 20383−20391.
26. Ohnishi, T.; Tamai, I.; Sakanaka, K.; Sakata, A.; Yamashima, T.; Yamashita, J.; Tsuji, A. In vivo and in vitro evidence for ATP-dependency of P-glycoprotein-mediated efflux of doxorubicin at the blood-brain barrier. *Biochem. Pharmacol*. **1995**, *49*, 1541−1544.
27. Gilman, A. G.; Rall, T. W.; Nies, A. S.; Taylor, P. *The pharmacological basis of therapeutics*; McGraw-Hill Book Co.: Singapore, 1991; pp 1811.
28. Sakata, A.; Tamai, I.; Kawazu, K.; Deguchi, Y.; Ohnishi, T.; Saheki, A.; Tsuji, A. *In vivo* evidence for ATP-dependent and P-glycoprotein-mediated transport of cyclosporin A at the blood-brain barrier. *Biochem. Pharmacol*. **1994**, *48*, 1989−1902.
29. Tamai, I.: Tsuji, A. Drug delivery through the blood-brain barrier. *Adv. Drug Deliv. Rev*. **1996**, *19*, 401−424.
30. Tsuji, A.; Tamai, I. Blood-brain barrier function of P-glycoprotein. *Adv. Drug Deliv. Rev*. **1997**, *19*, 287−298.

JS9901763